NUMERICAL SIMULATION OF MIXED CONVECTION FROM A CYLINDER IMMERSED IN VISCOPLASTIC FLUIDS

Daniel Dall'Onder dos Santos, dallonder@ufu.br

Federal University of Uberlândia, Av. João Naves de Ávila 2121, Uberlândia, MG, 38408-100, Brazil

Abstract: *The study of convection heat transfer involving viscoplastic fluids have raised a lot of attention in the recent years thanks to the huge economic importance on areas like the food, health care and oil industries, as well as biomedical engineering. Emulsions, suspensions and foams are common examples of this class of materials. From the heat transfer point of view, the abrupt changes in the viscosity presented by this class of fluids affects the flow field and consequently, the amount of thermal energy that can be carried by the fluid. In the other hand, the flow conditions around an immersed body can modify the heat transfer regime from or to forced, mixed and free convection. The relative importance of the forced and free convection contributions in the mixed convection regime is expressed using the Richardson number. This work aims to perform numerical simulations of non-isothermal two-dimensional steady state laminar flows over a cylinder immersed on viscoplastic fluids. The mechanical model is defined by the mass, momentum and energy balance equations coupled to the SMD equation to model the viscoplastic behavior. This modeling is approximated by a stabilized multi-field Galerkin finite element methodology, having as primal variables the velocity, pressure and extra-stress fields, coupled to a routine to calculate the temperature field. In the performed numerical simulations, the governing parameters, namely the power-law index, Herschel-Bulkley and Richardson numbers are varied in order to evaluate their influence on the cylinder heat transfer and drag coefficient.*
Keywords: *viscoplastic flow, mixed convection, finite element method, SMD model*

1. INTRODUCTION

The viscoplastic behavior is found in a wide range of engineering applications in the form of foams, emulsions and suspensions, e.g., food, toiletries, cosmetics, oil and building materials. The study of the fluid transport between reservoirs, containers and through pipelines is increasing in importance due to the value added of these products. On many applications, beyond the moving, there is the fluid heating or cooling. Very little is known about the heat transfer characteristics of viscoplastic materials and recent attention is being addressed in the literature to forced-, free- and mixed-convection heat transfer regimes. Soares *et al.* (1999) numerically analyzed the heat transfer in the entrance-region of tubes for Herschel-Bulkley fluid flows. The mechanical model was approximated via the finite volume method and the authors also used constant wall heat flux and constant wall temperature to investigate the effects of temperature-dependent properties. Altough not directly related to this work, once the viscosity funcion employed here does not model the temperature dependency, general results showed important differences on the heat transfer if the fluid is simulated as temperature-dependent. Presenting similar results, it is important to cite the paper of Nouar *et al.* (1995). The authors present a numerical analysis of the laminar forced convection in a cylindrical duct for a thermo-dependent Herschel-Bulkley fluid considering constant wall heat flux and constant wall temperature. The governing equations were solved using the finite difference method assuming all fluid properties constant except the consistency index constant. The authors obtained correlations for the local Nusselt number and the pressure gradient considering the temperature-dependent characteristic of the fluid. It is worthwhile to mention that the SMD viscosity function, proposed by de Souza Mendes and Dutra (2004) and used in this work, is very similar to the regularized Herschel-Bulkley equation when the Papanastasiou (1987) regularization is employed. A recent work which investigates the laminar forced convection of viscoplastic fluids is Nirmalkar *et al.* (2013) – the momentum and heat transfer characteristics of a heated square cylinder immersed in a streaming Bingham plastic medium were studied. The governing differential equations were solved numerically over wide ranges of Reynolds, Prandtl and Bingham numbers. The authors found that the unyielded regions expand with the increasing Bingham number and due to the yield stress, the drag force exerted by the fluid on the cylinder is higher than that in a Newtonian fluid at the same Reynolds number. Numerical results obtained for the drag and Nusselt numbers were correlated to modified Bingham and Reynolds numbers via expressions enabling their interpolation for intermediate values of the governing parameters. Similar researches were done by Shyam and Chhabra (2013) for tandem square cylinders immersed in power-law fluids and Tiwari and Chhabra (2015) for a semicircular cylinder immersed in Bingham fluids.

Some recent works found on literature focus its attention on an opposite way and investigated the free convection heat transfer in viscoplastic fluids. Sairamu *et al.* (2013) performed numerical simulations of Bingham fluids heat transfer from a heated horizontal circular cylinder in a square cavity using the finite-element based COMSOL solver, ranging the flow dimensionless parameters and the ratio between the cylinder diameter and the size of the square cavity. They found that as the size of the cavity increases with respect to the cylinder diameter, both Bingham and average Nusselt numbers increase. Free convection from a heated circular cylinder in Bingham fluid streams is investigated by Nirmalkar *et al.* (2014) ranging the Rayleigh, Prandtl and Bingham numbers. The authors observed the decrease in the yielded regions as the Bingham number is progressively increased or when the Rayleigh number is decreased as the buoyancy-induced flow weakens; the overall rate of heat transfer is determined by the gradients on the surface of the heated cylinder.

Coupling the two convection heat transfer mechanisms, Srinivas *et al.* (2009) numerically studied the mixed convection heat transfer from a cylinder in power-law fluids and found that both drag coefficient and average Nusselt number are augmented with the increasing buoyancy effects, Reynolds and Prandtl numbers. The increase in the shear-thinning tendency of the fluid enhances the drag and the heat transfer, whereas both of these are generally reduced in shear-thickening fluids. The buoyancy effects were found to be stronger in shear-thinning fluids and at low Reynolds number regimes. Nalluri *et al.* (2015) and Bose *et al.* (2015) simulated the mixed heat transfer in Bingham fluids for a heated hemisphere and a heated cylinder, respectively. Both studies observed that increasing Reynolds or Prandtl numbers tend to enhance convection and the size of the yielded regions have a positive dependence on these parameters. On the other hand, the Bingham and Richardson numbers tend to stabilize the flow by suppressing the propensity of flow detachment from the surface of the cylinder. The average Nusselt number and drag coefficient show a positive dependence on the Richardson number, but this dependence progressively weakens with the increasing Bingham number.

In this work, the mechanical model is numerically approximated by the finite element method for laminar mixed convection from a heated circular cylinder submerged in the stream of a non-Newtonian fluid. The power-law and the regularized Bingham fluid models are used in order to compare the employed methodology to the literature results. In a second step, the SMD fluid model is used to simulate the following range of conditions: the Richardson number from 0 to 2.5, the power-law index n from 0.25 to 1.25 and the Herschel-Bulkley number from 0.1 to 5000.

2. MECHANICAL MODEL

This work aims to study steady viscoplastic fluid flows around a heated cylinder kept in an infinite medium, as schematically shown in Fig. 1. Natural-, forced- or even mixed-convection is present once the fluid enters the flow domain with a given temperature lower than the cylinder temperature – the heat transfer regime depends on the prevailing flow conditions. In order to vary the fluid density with temperature, the Boussinesq approximation is used, given as $\rho = \rho_\infty[1 - \beta(T - T_\infty)]$, where β is the volumetric thermal expansion coefficient, T_∞ and ρ_∞ are the fluid temperature and density, respectively, imposed at the entrance of the flow domain.

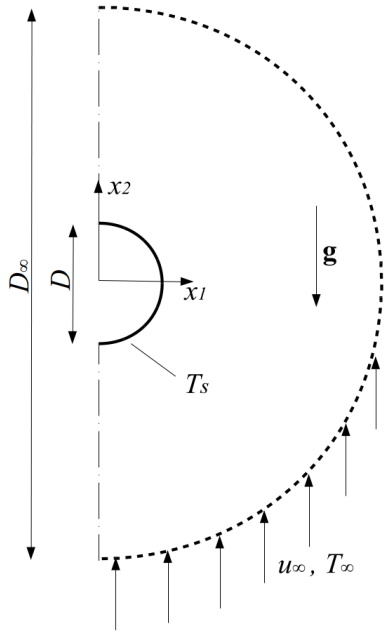

Figure 1: Sketch of the problem showing the employed boundary conditions.

The continuity, momentum balance, constitutive and energy equations, in a fixed Eulerian system, can be respectively expressed as

$$\begin{aligned}
&\rho_\infty \left(u_j \frac{\partial u_i}{\partial x_j} \right) = -\frac{\partial p}{\partial x_i} + \frac{\partial \tau_{ij}}{\partial x_j} + \rho_\infty g_i \beta (T - T_\infty), \\
&\frac{\partial u_i}{\partial x_i} = 0, \\
&\tau_{ij} = 2\eta(\dot{\gamma}) D_{ij}, \\
&\rho_\infty c_p \left(u_i \frac{\partial T}{\partial x_i} \right) = \kappa \left(\frac{\partial}{\partial x_i} \left(\frac{\partial T}{\partial x_i} \right) \right),
\end{aligned} \tag{1}$$

with

$$D_{ij} = \frac{1}{2} \left(\frac{\partial u_i}{\partial x_j} + \frac{\partial u_j}{\partial x_i} \right) \tag{2}$$

where u_i is the i component of the velocity vector, T is the temperature, p is the hydrostatic pressure, c_p and κ are respectively the fluid specific heat and thermal conductivity; g_i is the i component of the gravity vector – in this work, the gravity vector is aligned with the x_2 axis and hence $g_1 = 0$. τ_{ij} and D_{ij} are the ij component of the extra-stress and strain rate tensors, respectively.

Some assumptions are adopted to ease the numerical solution: the specific heat and thermal conductivity are constant, and the fluid viscosity does not depend on the temperature, only on the shear rate $\left(\dot{\gamma} = 2trD_{ij}{}^2)^{1/2}\right)$ according to the SMD viscosity model, proposed by de Souza Mendes and Dutra (2004) and modified by de Souza Mendes (2009). This modification was done to avoid a non-physical behavior of the viscosity, which could tend to zero as the shear rate increases. The SMD model becomes

$$\eta(\dot{\gamma}) = \left(1 - \exp\left(-\frac{\eta_0}{\tau_0}\dot{\gamma}\right)\right)\left(\frac{\tau_0}{\dot{\gamma}} + K\dot{\gamma}^{n-1}\right) + \eta_\infty \tag{3}$$

where η_0 and η_∞ are, respectively, the viscosities for very low and high values of the shear rate, τ_0 is the yield stress limit of the material, K is the consistency index, n is the power-law index, which controls the shear-thinning and shear-thickening of the fluid when the material starts to flow.

Alongside the SMD model, the power-law and the regularized Bingham model (Papanastasiou, 1987) are used in this work to perform the numerical code validation. They are written as

$$\begin{aligned}
\eta_{PL}(\dot{\gamma}) &= K\dot{\gamma}^{n-1} \\
\eta_{Bn}(\dot{\gamma}) &= \left(1 - \exp\left(-m\dot{\gamma}\right)\right)\frac{\tau_0}{\dot{\gamma}} + \mu_b
\end{aligned} \tag{4}$$

where μ_b is referred in the literature as the Bingham plastic viscosity, m is a numerical parameter; the remaining parameters are defined as previously.

2.1 Dimensionless Parameters

In order to obtain the mechanical problem in a non-dimensional form, the following set of dimensionless quantities must be introduced:

$$x_i^* = \frac{x_i}{D}\,,\ u_i^* = \frac{u_i}{u_\infty}\,,\ \tau_{ij}^* = \frac{\tau_{ij}}{K}\left(\frac{D}{u_\infty}\right)^n,\ p^* = \frac{p}{\rho_\infty u_\infty^2}\,,\ T^* = \frac{T - T_\infty}{T_s - T_\infty}\,,\ \eta^* = \frac{\eta}{K}\left(\frac{D}{u_\infty}\right)^{n-1},\ \dot{\gamma}^* = \dot{\gamma}\frac{D}{u_\infty} \tag{5}$$

where D is the cylinder diameter, u_∞ is the velocity imposed at the entrance of the flow domain and T_s is the cylinder surface temperature. Employing the above definitions, the mechanical model and the SMD viscosity equation becomes

$$\begin{aligned}
&u_j^*\frac{\partial u_i^*}{\partial x_j^*} = -\frac{\partial p^*}{\partial x_i^*} + \frac{K}{\rho_\infty u_\infty^{2-n} D^n}\frac{\partial \tau_{ij}^*}{\partial x_j^*} + \frac{g_i\beta(T_s - T_\infty)D}{u_\infty^2}T^*, \\
&\frac{\partial u_i^*}{\partial x_i^*} = 0, \\
&\tau_{ij}^* = 2\eta^*(\dot{\gamma}^*)D_{ij}^*, \\
&u_i^*\frac{\partial T^*}{\partial x_i^*} = \frac{K}{\rho_\infty u_\infty^{2-n} D^n}\frac{\kappa}{c_p K}\left(\frac{D}{u_\infty}\right)^{n-1}\left(\frac{\partial}{\partial x_i^*}\left(\frac{\partial T^*}{\partial x_i^*}\right)\right), \\
&\eta^*(\dot{\gamma}^*) = \left(1 - \exp\left(-\frac{\eta_0 u_\infty}{\tau_0 D}\dot{\gamma}^*\right)\right)\left(\frac{\tau_0}{K}\left(\frac{D}{u_\infty}\right)^n\frac{1}{\dot{\gamma}^*} + \dot{\gamma}^{*n-1}\right) + \frac{\eta_\infty}{K}\left(\frac{D}{u_\infty}\right)^{n-1}
\end{aligned} \tag{6}$$

The non-dimensional parameters commonly found on the non-Newtonian literature (e.g., Jay *et al.* (2001), Alexandrou *et al.* (2003), Neofytou and Drikakis (2003), de Souza Mendes *et al.* (2007), de Souza Mendes (2007), Sahu *et al.* (2010), Siqueira (2013), and references therein) are the power-law Reynolds, the Herschel-Bulkley and the jump numbers, the power-law Prandtl and the Richardson numbers, respectively given as

$$\begin{aligned}
&Re_{PL} = \frac{\rho_\infty u_\infty^{2-n} D^n}{K},\ HB = \frac{\tau_0}{K}\left(\frac{D}{u_\infty}\right)^n,\ J = \frac{\eta_0 \tau_0^{(1-n)/n}}{K^{1/n}} - 1 \\
&Pr_{PL} = \frac{c_p K}{\kappa}\left(\frac{u_\infty}{D}\right)^{n-1},\ Ri = \frac{|\mathbf{g}|\beta(T_s - T_\infty)D}{u_\infty^2}
\end{aligned} \tag{7}$$

Aplying the above definitions on Eq. (6), the non-dimensional mechanical model becomes

$$
\begin{aligned}
& u_j^* \frac{\partial u_i^*}{\partial x_j^*} = -\frac{\partial p^*}{\partial x_i^*} + \frac{1}{Re_{PL}} \frac{\partial \tau_{ij}^*}{\partial x_j^*} + RiT^*, \\
& \frac{\partial u_i^*}{\partial x_i^*} = 0, \\
& \tau_{ij}^* = 2\eta^*(\dot{\gamma}^*) D_{ij}^*, \\
& u_i^* \frac{\partial T^*}{\partial x_i^*} = \frac{1}{Re_{PL} Pr_{PL}} \left(\frac{\partial}{\partial x_i^*} \left(\frac{\partial T^*}{\partial x_i^*} \right) \right), \\
& \eta^*(\dot{\gamma}^*) = \left(1 - \exp\left(-\frac{J+1}{HB^{1/n}} \dot{\gamma}^* \right) \right) \left(\frac{HB}{\dot{\gamma}^*} + \dot{\gamma}^{*n-1} \right) + \eta_\infty^*
\end{aligned}
\tag{8}
$$

3. NUMERICAL SOLUTION METHODOLOGY

In this work, the numerical approximation of the mechanical model is done employing the finite element method. A stabilized multi-field Galerkin least-squares formulation in terms of velocity, pressure and extra-stress is used to solve the fluid mechanical behavior (NNFEM routine) – see Zinani (2006), Zinani and Frey (2006), Zinani and Frey (2008), Frey *et al.* (2010) and Santos *et al.* (2011) for further details. This formulation is a direct extension of the one introduced by Behr et al., 1993, for constant viscosity fluids, to perform numerical simulations of non-Newtonian fluid flows. The thermal field is calculated in a separated routine (FEM90). In all calculations, it is used equal-order bi-linear (Q1) finite element interpolations.

The solution is obtained from initial velocity and temperature guesses (e.g., an isothermal Newtonian flow). After the convergence of the two routines, the error calculated between to consecutive algorithm iterations for all the variables is evaluated – as depicted in the solution algorithm flow chart (Fig. 2). If the maximum error value is lower than 10^{-6}, the resullt is stored and post-processed.

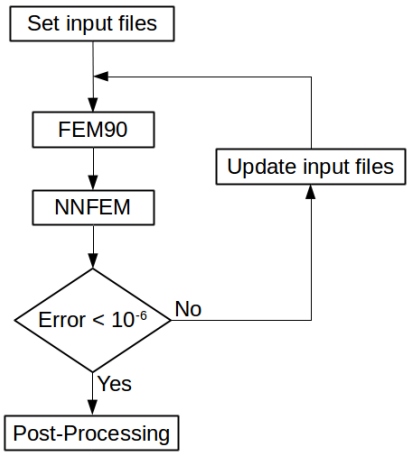

Figure 2: Solution algorithm flow chart.

4. RESULTS

This section presents the results obtained with the aforementioned formulation for non-isothermal two-dimensional steady state laminar flows over a cylinder immersed on viscoplastic fluids. As briefly discussed in Section 2 and schematically shown on Fig. 1, the boundary conditions imposed over the geometry are similar to that used by Bose *et al.* (2015). Also, it is supposed that whitin the power-law Reynolds number range simulated in this work, the flow is symmetric and only half geometry is considered. The cylinder surface is assumed impermeable ($u_1 = u_2 = 0$) at the given temperature T_s. In the symmetry line, it is used the usual $\tau_{12}^* = 0$ and $u_1^* = 0$ conditions. At the flow external boundary (D_∞), it is imposed $u_1^* = 0$, $u_2^* = 1$ and T_∞ along the lower half; on the upper half, only $u_1^* = 0$.

The mesh independence procedure is done alongside the analysis of the results presented by Srinivas *et al.* (2009) and Bose *et al.* (2015), respectively for power-law and Bingham fluid flows, and shown on Tab. 1. Only two different domain discretizations are used in this work: D1, with 4800 bilinear Lagrangian (Q1) elements and D2, with 6400 elements. Even D1 and D2 being very coarse meshes, the error when the drag coefficient and the average Nusselt number (defined as in Srinivas *et al.* (2009)) are compared is relatively low – from 0.14% to 2.0% for C_D and from 0.6% to 3.2% for $\overline{Nu}_D$. It is important to keep in mind how these two quantities are strongly bound to the pressure, stress, velocity and temperature fields. When the error for the results obtained using the D1 and D2 meshes for C_D and $\overline{Nu}_D$ is compared, the coarser mesh presents better results in some cases. Altough this unusual trend, D2 was selected to perform the numerical simulations as it is capable to represent smootly the flow unyielded regions.

Is also worthwhile to remark the ratio between D_∞, the diameter of the fluid domain and D, the cylinder diameter. As cited by several authors, the distance between the solid surface and the flow boundary need to be sufficiently large to ensure that there is no influence over the flow and temperature fields at the vicinity of the cylinder. In this work, it is employed a small D_∞/D ratio equal to 100 – Srinivas *et al.* (2009) employed 1200 for flows with $Re_{PL} < 5$, and 300 for $Re_{PL} \geq 5$; Bose *et al.* (2015) employed 1000 for all flows. Certainly this fact adds some numerical errors and collaborates with the discrepancies between the results obtained in this work and and prior studies.

Table 1: Comparison of the present results with different mesh refinements and prior studies.

Power-law fluid – $Re_{PL} = 5$, $Pr_{PL} = 100$, $n = 0.2$ and $Ri = 0$										
–	Srinivas *et al.* (2009)		Present Work – D1		Error (%)		Present Work – D2		Error (%)	
	C_D	Nu	C_D	Nu	C_D	Nu	C_D	Nu	C_D	Nu
	5.7693	11.2669	5.7779	11.1996	0.151	0.597	5.7772	11.3404	0.138	0.653
Power-law fluid – $Re_{PL} = 1$, $Pr_{PL} = 100$, $n = 0.6$ and $Ri = 2$										
–	Srinivas *et al.* (2009)		Present Work – D1		Error (%)		Present Work – D2		Error (%)	
	C_D	Nu	C_D	Nu	C_D	Nu	C_D	Nu	C_D	Nu
	22.5131	4.4097	22.0567	4.2950	2.026	2.601	22.0516	4.3270	2.050	1.876
Bingham fluid – $Re_{Bn} = 0.1$, $Pr_{Bn} = 1$, $Bn = 10$ and $m = 10^5$										
	Bose *et al.* (2015)		Present Work – D1		Error (%)		Present Work – D2		Error (%)	
Ri	C_D	Nu	C_D	Nu	C_D	Nu	C_D	Nu	C_D	Nu
0	3255	0.5057	3250.0	0.5179	0.154	2.415	3249.5	0.5220	0.168	3.233
2	3254.8	0.5062	3248.6	0.5179	0.192	2.314	3248.1	0.5220	0.207	3.131

4.1 Validation of the results: power-law fluid model

Table 2 and Tab. 3 show the comparison with Srinivas *et al.* (2009) for flow regimes with $Ri = 0$ and 2, respectively. The power-law Reynolds number was varied from 1 to 40, the power-law index form 0.2 to 1.8, the Prandtl number is kept equal to 100 for both Richardson numbers considered. The authors discretized their computational domain using 505200 volumes for flows with $Re_{PL} < 5$, and 134200 volumes for $Re_{PL} \geq 5$. The major discrepancies are observed for the lower Reynolds and lower n index, where the error reaches 5.71% on the average Nusselt number. Another remark must be made on the different trend between the Richardson numbers – $Ri = 0$ presents the larger errors in $\overline{Nu}_D$ while $Ri = 2$ presents the larger errors in C_D.

Table 2: Comparison of the present results and prior studies with the power-law model, for $Ri = 0$.

-		Srinivas *et al.* (2009)		Present Work		Error (%)	
Re	n	C_D	Nu	C_D	Nu	C_D	Nu
1	0.2	26.7718	5.6551	26.9044	5.9780	0.495	5.710
	1.8	5.8382	3.1103	5.8187	3.087	0.335	0.735
5	0.2	5.7693	11.2669	5.772	11.3404	0.138	0.653
	1.8	3.2219	5.8194	3.2128	5.7764	0.282	0.739
40	0.2	1.1391	29.7471	1.1205	30.4485	1.629	2.358
	1.8	1.6620	15.6635	1.6603	15.7389	0.099	0.481

Table 3: Comparison of the present results and prior studies with the power-law model, for $Ri = 2$.

-		Srinivas *et al.* (2009)		Present Work		Error (%)	
Re	n	C_D	Nu	C_D	Nu	C_D	Nu
1	0.6	22.5131	4.4097	22.0516	4.3270	2.050	1.876
	1.0	16.7803	3.8286	16.4442	3.7785	2.003	1.308
	1.8	12.3303	3.5715	12.1743	3.5395	1.265	0.897
5	1.0	6.1710	7.6219	6.1620	7.5664	0.146	0.728
	1.8	5.7618	6.7627	5.7727	6.7171	0.190	0.674
40	0.2	1.4510	39.6514	1.4247	39.7987	1.812	0.372
	1.0	2.308	19.9606	2.2938	19.7037	0.613	1.287

4.2 Validation of the results: Bingham fluid model

The comparison with Bose *et al.* (2015) is shown in Tab. 4 for $Re_{Bn} = \rho u_\infty D/\mu_b = 0.1$, $Pr_{Bn} = c_p\mu_b/\kappa = 1$, and $Bn = 10$, also for Richardson numbers equal to 0 and 2 for two values of the m index: 10^5 and 10^6. This numeric

parameter was introduced by Papanastasiou (1987) to regularize the Bingham model – although it does not have a physical meaning. For all simulations, the authors employed a computational domain with 48000 elements. The results from a same m index varying the Ri number have little or no noticeable difference on the C_D and $\overline{Nu}_D$. From its physical interpretation, the Richardson number is a ratio between natural convection and forced convection – or even between buoyancy and inertia forces if the relation $Ri = Gr/Re^2$ is kept in mind. From this point of view, whilst there is a Ri variation, the Grashof number will be low if the Reynolds number is low. The effect of the buoyancy aiding the inertia force to overcome the viscous force, even in a mixed-convection condition, will barely be noticeable.

Table 4: Comparison of the present results and prior studies with the Bingham model.

-		Bose *et al.* (2015)		Present Work		Error (%)	
Ri	m	C_D	Nu	C_D	Nu	C_D	Nu
0	10^5	3255.0	0.5057	3249.52	0.522	0.168	3.233
	10^6	3262.1	0.5165	3249.53	0.522	0.385	1.075
2	10^5	3254.8	0.5062	3248.05	0.522	0.207	3.131
	10^6	3261.8	0.5166	3248.06	0.522	0.421	1.055

4.3 Results with the SMD fluid model

This section presents the results obtained using the modified SMD viscoplastic model (Eq. 3). Figure 3 shows the effect of the Richardson number on C_D and $\overline{Nu}_D$, for Re_{PL}=10, Pr_{PL}=1, HB=10, n=0.5 and J=10^6. As expected, the heat transfer is enhanced almost linearly with the aid of the natural convection, once the velocity imposed by the boundary condition is in the opposite direction of the gravity vector. When comparing the simulation for Ri=2.5 with the forced convection situation, the increase in C_D is about 6.7% and in $\overline{Nu}_D$ about 4.6%.

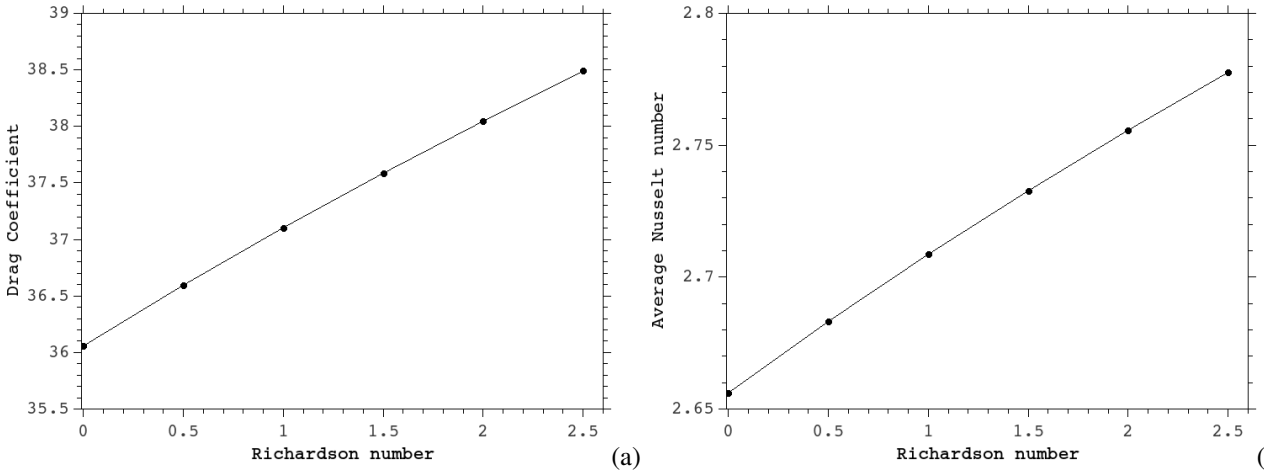

(a) (b)

Figure 3: The drag coefficient (a) and average Nusselt number (b) for Re_{PL}=10, Pr_{PL}=1, HB=10, n=0.5 and J=10^6.

The employed nondimensionalization, presented in Eq. (7), couples rheological and kinematic properties. To perform the evaluation of the power-law index and Herschel-Bulkley number influence on the heat transfer, attention must be paid to the set of non-dimensional variables which are originated – only the Richardson number is not affected when the n and HB variations are performed and some representative values are shown in Tab. 5.

Table 5: Dimensionless parameters for n index and HB variation.

n index variation					HB variation	
n	Re_{PL}	Pr_{PL}	HB	J	HB	J
0.25	17.78	0.56	17.78	1.10^9	1	1.10^5
0.50	10	1.0	10	1.10^6	10	1.10^6
0.75	5.62	1.78	5.62	1.10^5	100	1.10^7
1.00	3.16	3.16	3.16	3.16^4	1000	1.10^8
1.25	1.78	5.62	1.78	1.58^4	5000	5.10^8

The power-law index is an important rheological property, which determines the decrease or increase of the viscosity when the fluid begins to flow ($\tau > \tau_0$). The influence of this parameter is shown on Figure 4. For n=0.25, the shear-thinning effect becomes very clear, once it is observed the lower value for the drag coefficient and higher average Nusselt number. As the n index is enlarged, the fluid becomes increasingly thick and there is more opposition to the fluid motion – C_D is 55% higher when comparing with n=0.25 and n=1.25. With the increasing viscosity and its direct effect on the convection heat transfer, there is a reduction of 15% in the $\overline{Nu}_D$ for the same ranged values.

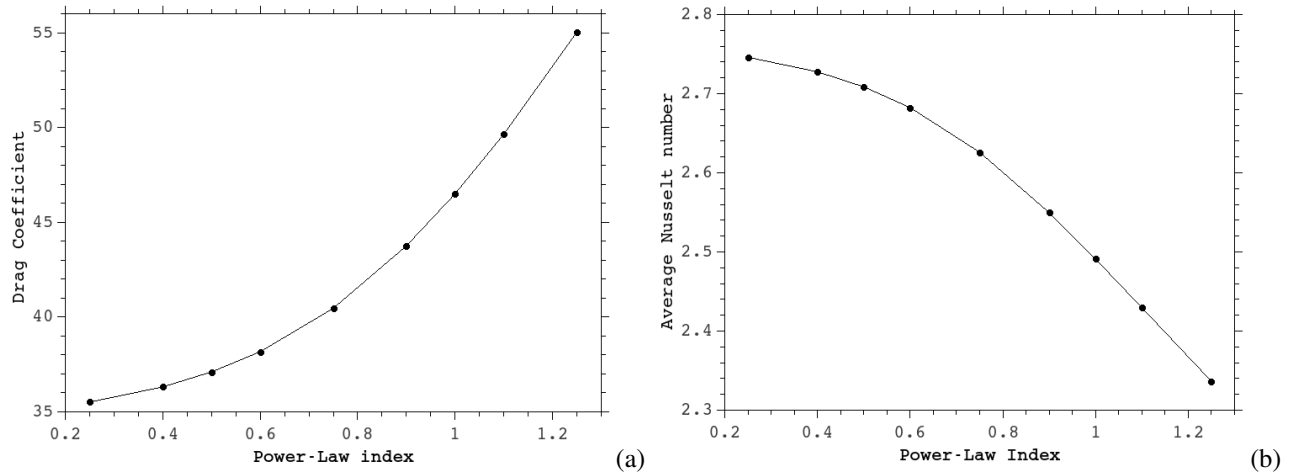

(a) (b)

Figure 4: The drag coefficient (a) and average Nusselt number (b) for Ri=1.

The Herschel-Bulkley number is an interesting parameter once it relates the yield stress with kinematic and geometric quantities. In this way, it can be considered as a measure of the viscoplasticity level of the fluid flow and has strong effects on the drag coefficient, another expected trend. The C_D grows rapidly as the HB number is increased – depicted in Fig. 5(a). On the other hand, the Nusselt number increases for HB numbers between 0.1 and 500 and has an abrupt decrease for the larger values simulated. This behavior is better understood when the vertical velocity (u_2^*) profiles at x_2^*=0 are taken into account – Fig. 6. The higher shear rates of the entire flow domain are on the vicinity of the cylinder. The fluid acceleration and deceleration to surpass the obstructing object is facilitated by the viscosity drop next to the solid surface – which becomes more accented as the HB number is increased until the value of 500. However, for HB>500, the flow viscoplasticity is so intense that even the high shear rates regions are affected: the fluid flows slower near to the cylinder and the convection heat transfer is decreased. Figure 7 shows some of the unyielded regions obtained for the Herschel-Bulkley number variation. They increase monotonically as HB is increased due to the lower level of stresses that tends to break the material structure.

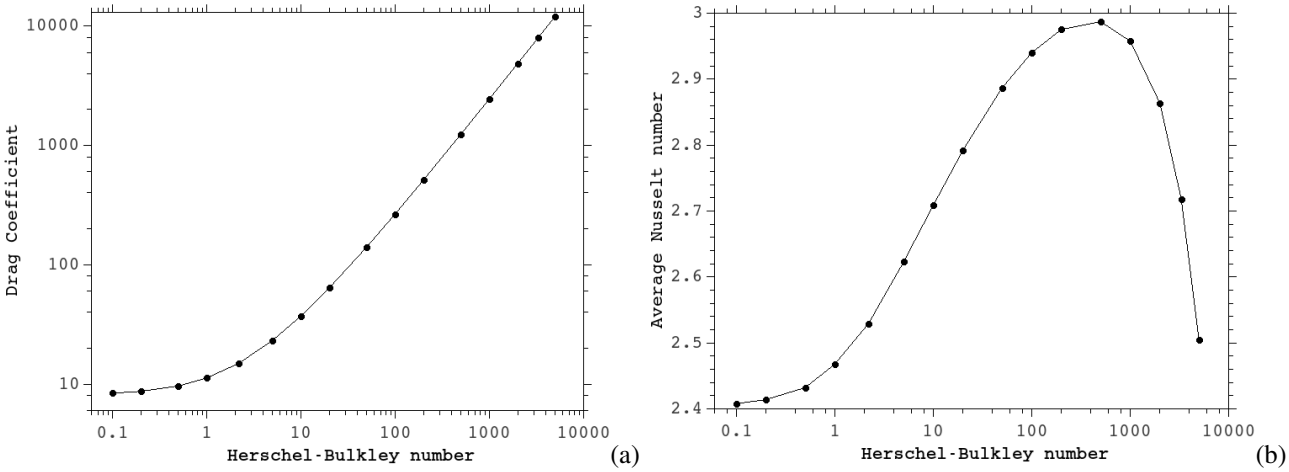

(a) (b)

Figure 5: The drag coefficient (a) and average Nusselt number (b) for Re_{PL}=10, Pr_{PL}=1, Ri=1 and n=0.5.

5. FINAL REMARKS

This work presents numerical results obtained for non-Newtonian fluid flows around an immersed heated cylinder. The flow dimensionless parameters, namely the Richardson number, the power-law index and the Herschel-Bulkley number, were varied in order to evaluate the capability of heat exchange between the cylinder and the fluid. The effect over the drag coefficient is also evaluated and the increase of the Ri and HB numbers, as well as the increase in the n index, affects positively the C_D. From the heat transfer point of view, the aid of natural convection has a positive effect over the average Nusselt number – the opposite behavior is observed with the increase of the power-law index, as the fluid becomes ticker and the advection transport is reduced. The flow viscoplastic level, measured by the HB number, has two effects over the heat transfer. For a range of $HB < 500$, the Nusselt number is increased due to the acceleration of the fluid near the cylinder surface. This region presents the higher shear rates of the entire flow field. For $HB > 500$, even the cylinder vicinity is under strong viscoplastic effects – the flow is decelerated and the advection heat transport is diminished. It is also important to mention the stability of the solution methodology based on a finite element formulation providing satisfactory results even for coarse meshes, as is shown by the comparison with literature results.

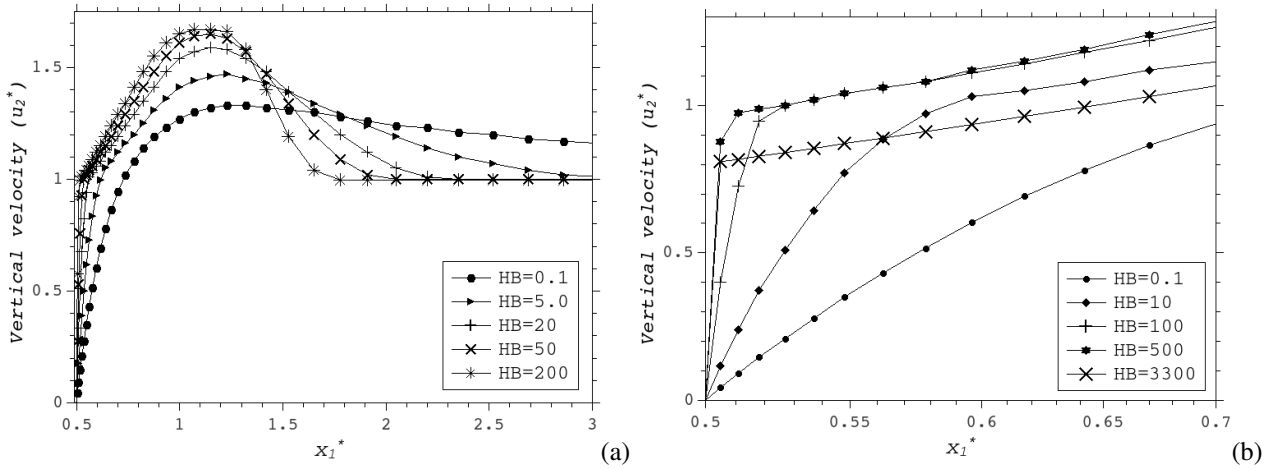

Figure 6: Velocity profiles (u_2^*) for Re_{PL}=10, Pr_{PL}=1, Ri=1 and n=0.5, ranging the HB number. (a) profiles spanning a distance of 2.5D from the cylinder surface for HB<500; (b) a detailed view at the cylinder vicinity.

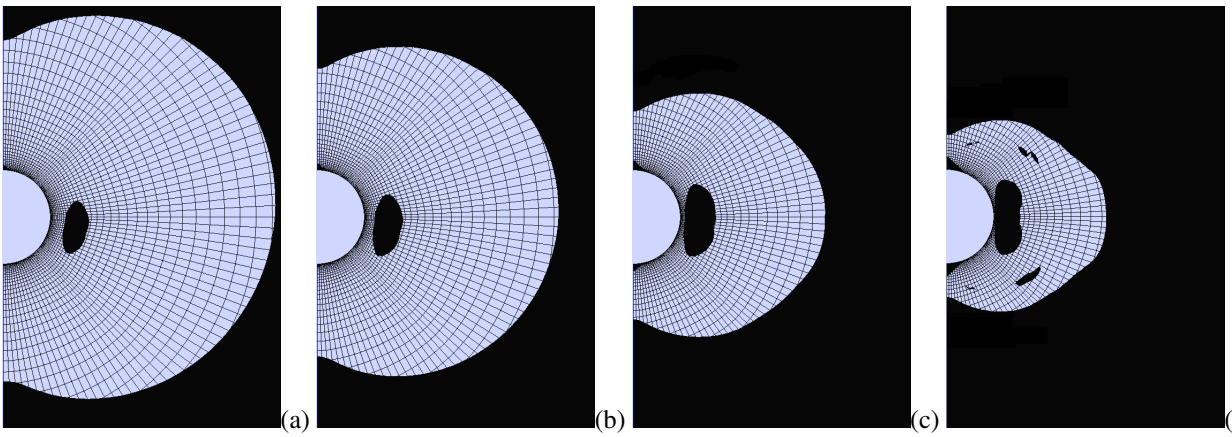

Figure 7: Unyielded regions obtained via the $|\tau| < \tau_0$ criterion (Mitsoulis and Zisis, 2001) for the Herschel-Bulkley variation: (a) HB=5; (b) HB=10; (c) HB=50; (d) HB=500.

6. ACKNOWLEDGEMENTS

The author acknowledge FAPEMIG and the Faculty of Mechanical Engineering (FEMEC/UFU) for financial support.

7. REFERENCES

Alexandrou, A.N., Le Menn, P., Georgiou, G. and Entov, V., 2003. "Flow instabilities of Herschel–Bulkley fluids". *Journal of Non-Newtonian Fluid Mechanics*, Vol. 116, pp. 19–32.

Bose, A., Nirlmalkar, N. and Chhabra, R.P., 2015. "Effect of aiding-buoyancy on mixed-convection from a heated cylinder in Bingham plastic fluids". *Journal of Non-Newtonian Fluid Mechanics*, Vol. 220, pp. 3–21.

de Souza Mendes, P.R., 2007. "Dimensionless non-Newtonian fluid mechanics". *Journal of Non-Newtonian Fluid Mechanics*, Vol. 147, pp. 109–116.

de Souza Mendes, P.R., 2009. "Modeling the thixotropic behavior of structured fluids". *Journal of Non-Newtonian Fluid Mechanics*, Vol. 164, pp. 66–75.

de Souza Mendes, P.R. and Dutra, E.S.S., 2004. "Viscosity function for yield-stress liquids". *Applied Rheology*, Vol. 14, pp. 296–302.

de Souza Mendes, P.R., Naccache, M.F., Varges, P.R. and Marchesini, F.H., 2007. "Flow of viscoplastic liquids through axisymmetric expansions-contractions". *Journal of Non-Newtonian Fluid Mechanics*, Vol. 142, pp. 207–217.

Frey, S.L., Silveira, F.S. and Zinani, F.S.F., 2010. "Stabilized mixed approximations for inertial viscoplastic fluid flows". *Mechanics Research Communications*, Vol. 37, pp. 145–152.

Jay, P., Magnin, A. and Piau, J.M., 2001. "Viscoplastic fluid flow through a sudden axisymmetric expansion". *AIChE Journal*, Vol. 47, No. 10, pp. 2155–2166.

Mitsoulis, E. and Zisis, T., 2001. "Flow of bingham plastics in a lid-driven square cavity". *Journal of Non-Newtonian Fluid Mechanics*, Vol. 101, pp. 173–180.

Nalluri, S.V., Patel, S.A. and Chhabra, R., 2015. "Mixed convection from a hemisphere in bingham plastic fluids". *International Journal of Heat and Mass Transfer*, Vol. 84, pp. 304–318.

Neofytou, P. and Drikakis, D., 2003. "Non-newtonian flow instability in a channel with a sudden expansion". *Journal of Non-Newtonian Fluid Mechanics*, Vol. 111, pp. 127–150.

Nirmalkar, N., Bose, A. and Chhabra, R.P., 2014. "Free convection from a heated circular cylinder in bingham plastic fluids". *International Journal of Thermal Sciences*, Vol. 83, pp. 33–44.

Nirmalkar, N., Chhabra, R.P. and Poole, R.J., 2013. "Laminar forced convection heat transfer from a heated square cylinder in a bingham plastic fluid". *International Journal of Heat and Mass Transfer*, Vol. 56, pp. 625–639.

Nouar, C., Lebouché, M., Devienne and Riou, C., 1995. "Numerical analysis of the thermal convection for herschel-bulkley fluids". *International Journal of Heat and Fluid Flow*, Vol. 13, pp. 223–232.

Papanastasiou, T.C., 1987. "Flow of materials with yield". *Journal of Rheology*, Vol. 31, pp. 385–404.

Sahu, A.K., Chhabra, R.P. and Eswaran, V., 2010. "Two-dimensional laminar flow of a power-law fluid across a confined square cylinder". *Journal of Non-Newtonian Fluid Mechanics*, Vol. 165, pp. 752–763.

Sairamu, M., Nirmalkar, N. and Chhabra, R., 2013. "Natural convection from a circular cylinder in confined bingham plastic fluids". *International Journal of Heat and Mass Transfer*, Vol. 60, pp. 567–581.

Santos, D.D., Frey, S.L., Naccache, M.F. and de Souza Mendes, P.R., 2011. "Numerical approximations for flow of viscoplastic fluids in a lid-driven cavity". *Journal of Non-Newtonian Fluid Mechanics*, Vol. 166, pp. 667–679.

Shyam, R. and Chhabra, R.P., 2013. "Effect of prandtl number on heat transfer from tandem square cylinders immersed in power-law fluids in the low reynolds number regime". *International Journal of Heat and Mass Transfer*, Vol. 57, pp. 742–755.

Siqueira, E.S., 2013. *Aproximação numérica de escoamentos de fluidos power-law utilizando o código livre Mfix*. Master's thesis, Programa de Pós Graduação em Engenharia Mecânica da Universidade do Vale do Rio dos Sinos – UNISINOS.

Soares, M., Naccache, M.F. and de Souza Mendes, P.R., 1999. "Heat transfer to viscoplastic materials flowing laminarly in the entrance region of tubes". *International Journal of Heat and Fluid Flow*, Vol. 20, pp. 60–67.

Srinivas, A.T., Bharti, R.P. and Chhabra, R.P., 2009. "Mixed convection heat transfer from a cylinder in power-law fluids: effect of aiding buoyancy". *Industrial & Engineering Chemistry Research*, Vol. 48, pp. 9735–9754.

Tiwari, A.K. and Chhabra, R.P., 2015. "Momentum and heat transfer from a semi-circular cylinder in bingham plastic fluids". *Applied Mathematical Modelling*, Vol. 39, pp. 7045–7064.

Zinani, F.S.F., 2006. *Desenvolvimento e Implementação Computacional de Formulações Galerkin Mínimos-Quadrados para Escoamentos Não-Newtonianos Sensíveis à Cinemática*. Ph.D. thesis, Programa de Pós Graduação em Engenharia Mecânica da Universidade Federal do Rio Grande do Sul – UFRGS.

Zinani, F.S.F. and Frey, S.L., 2006. "Galerkin least-squares finite element approximations for isochoric flows of viscoplastic liquids". *Journal of Fluids Engineering*, Vol. 128, No. 4, pp. 856–863.

Zinani, F.S.F. and Frey, S.L., 2008. "Galerkin least-squares multifield approximations for flows of inelastic non-newtonian fluids". *Journal of Fluids Engineering*, Vol. 130, pp. 1–14.

8. RESPONSIBILITY NOTICE

The author is the only responsible for the printed material included in this paper.